Molecules and Cells

# The Kleisin Subunits of Cohesin Are Involved in the Fate Determination of Embryonic Stem Cells

Young Eun Koh[1,2], Eui-Hwan Choi[1,3], Jung-Woong Kim[1,*], and Keun Pil Kim[1,*]

[1]Department of Life Sciences, Chung-Ang University, Seoul 06974, Korea, [2]Genexine Inc., Bio Innovation Park, Seoul 07789, Korea, [3]New Drug Development Center, Daegu-Gyeongbuk Medical Innovation Foundation, Daegu 41061, Korea
*Correspondence: jungkim@cau.ac.kr (JWK); kpkim@cau.ac.kr (KPK)
https://doi.org/10.14348/molcells.2022.2042
www.molcells.org

**As a potential candidate to generate an everlasting cell source to treat various diseases, embryonic stem cells are regarded as a promising therapeutic tool in the regenerative medicine field. Cohesin, a multi-functional complex that controls various cellular activities, plays roles not only in organizing chromosome dynamics but also in controlling transcriptional activities related to self-renewal and differentiation of stem cells. Here, we report a novel role of the α-kleisin subunits of cohesin (RAD21 and REC8) in the maintenance of the balance between these two stem-cell processes. By knocking down REC8, RAD21, or the non-kleisin cohesin subunit SMC3 in mouse embryonic stem cells, we show that reduction in cohesin level impairs their self-renewal. Interestingly, the transcriptomic analysis revealed that knocking down each cohesin subunit enables the differentiation of embryonic stem cells into specific lineages. Specifically, embryonic stem cells in which cohesin subunit RAD21 were knocked down differentiated into cells expressing neural alongside germline lineage markers. Thus, we conclude that cohesin appears to control the fate determination of embryonic stem cells.**

**Keywords:** cohesin, embryonic stem cells, RAD21, REC8, trascriptomic analysis

## INTRODUCTION

Controlled differentiation of embryonic stem cells (ESCs) to specific lineages has long been considered innovative in the field of regenerative medicine, with the merit that they may serve as an everlasting cell source to treat debilitating diseases once considered incurable (Keller, 2005; Murry and Keller, 2008; Sobhani et al., 2017). However, the major challenge in this strategy is the generation of physiological cells (Efthymiou et al., 2014; Findikli et al., 2006; Gorecka et al., 2019).

ESCs are pluripotent cells, which can differentiate into every cell type in the embryo and have the ability of self-renewal (Subramanian et al., 2009; Walker et al., 2007; Zakrzewski et al., 2019). Thus, these cells have been regarded as a promising therapeutic tool against various degenerative diseases, but the mechanisms underlying these two properties of ESCs are still under investigation (Heng et al., 2004; Vazin and Freed, 2010; Young, 2011). Therefore, a comprehensive approach to understanding these mechanisms is essential to harness the pluripotency of ESCs for clinical applications. In the past decades, many studies have focused on strategies that control the expression of genes related to ESC self-renewal, and increasing evidence suggests a role of cohesin in ESC differentiation (Cuartero et al., 2018; Kagey et al., 2010; Noutsou et al., 2017).

As eukaryotic cells have distinct time gaps between the time of chromosome duplication and segregation, cell division must be strictly regulated to distribute one copy of each duplicated chromosome to each daughter cell (Brooker and Berkowitz, 2014; Choi et al., 2017; Mehta et al., 2012). The cohesin complex is known to be essential for the accurate

Received 9 December, 2021; revised 20 June, 2022; accepted 24 July, 2022; published online 28 September, 2022

eISSN: 0219-1032

distribution of chromosomes to daughter cells. Regarded as a "molecular glue," cohesin uses its tripartite ring-shaped structure to entrap the duplicated chromosome until anaphase (Peters et al., 2008). This protein complex is composed of four core subunits, which include the structural maintenance of chromosomes (SMC) proteins SMC1A and SMC3, the kleisin protein RAD21, and the stromal antigen (SA) protein SA1/STAG1 or SA2/STAG2 (Nasmyth and Haering, 2009). In addition, mammalian meiosis-specific cohesin components, which include SMC1β, RAD21L, REC8, and SA3/STAG3 (Biswas et al., 2016; Choi et al., 2022; Hong et al., 2019; Ishiguro, 2019). Recently, Choi et al. (2022) have demonstrated that the components of meiosis-specific cohesin are expressed in ESCs as well and play a role in the chromosomal organization and sister-chromatid cohesion. Given that the cohesin complex has diverse roles in organizing chromosome dynamics and transcriptional activities related to ESC self-renewal and differentiation (Kagey et al., 2010; Noutsou et al., 2017), it is truly positioned as a multi-functional complex that controls various cellular activities. Although the role of cohesin in chromosome dynamics has been well studied (Han et al., 2021; Hirano, 2015; Revenkova et al., 2004), its role in regulating ESC differentiation remains unclear.

In this study, we reveal that cohesin may function to maintain the balance between ESC self-renewal and differentiation. Based on the RNA-sequencing data, we determined that knocking down each cohesin factor not only accelerated the differentiation of ESCs but also induced their differentiation into specific lineages. We used four transcriptional factors known to be essential for maintaining the pluripotency of ESCs—Oct4 (Pou5f1), Nanog, Sox2, and Klf4 (Takahashi and Yamanaka, 2006). By using these transcriptional factors, we observed reduced expression of cohesin accelerated differentiation of ESC when compared with the control group. We then examined the lineage of the differentiated cells by characterizing their expression patterns of specific markers commonly used for lineage determination. Accordingly, knocking down cohesin subunits induced ESC differentiation into diverse cell types with markers of specific lineages. Harnessing this ability of cohesin can provide new approaches for controlled differentiation of ESCs and new insights for regenerative medicine and tissue engineering.

## MATERIALS AND METHODS

### Cell lines

The J1 mouse ESCs were derived from the inner cell mass of a male agouti 129S4/SvJae embryo. These cells (mESCs) were used in all the experiments presented in this article. mESCs were maintained in DMEM High Glucose (10566016; Gibco, USA) with 10% horse serum (16050122; Gibco), 2 mM L-glutamine (25030081; Gibco), 10 mM HEPES (15630080; Gibco), 0.1 mM beta-mercaptoethanol (31350010; Gibco), 0.1 mM MEM Non-Essential Amino Acids (11140050; Gibco), 100 U/ml penicillin-streptomycin (10378016; Gibco), and $10^3$ U/ml ESGRO Recombinant Mouse Leukemia Inhibitory Factor (LIF) (ESG1107; Millipore, USA). Cells were cultured in a humidified 5% $CO_2$ incubator at 37°C.

### Stem cell differentiation

Individual cultured cells were used for the sample preparation. mESCs were differentiated in DMEM High Glucose (10566016) with 10% horse serum (16050122), 2 mM L-glutamine (25030081), 10 mM HEPES (15630080), 0.1 mM beta-mercaptoethanol (31350010), 0.1 mM MEM Non-Essential Amino Acids (11140050), 100 U/ml penicillin-streptomycin (10378016) for 96 h. LIF was excluded in culture media to induce differentiation of mESCs.

### RNA extraction

RNA sample used in this study was extracted using RNeasy Mini Kit (74104; Qiagen, Germany). Total RNA was purified from mESCs. After cell lysis and homogenization, the lysates were loaded onto the RNeasy silica membrane. Any residual DNA was removed through on-column DNase treatment. Purified RNA was eluted using RNase-free DEPC water. All the procedures followed the directions of the manufacturers. RNA quality and quantity were assessed using an Agilent 2100 Bioanalyzer (Agilent Technologies, The Netherlands) and ND-2000 Spectrophotometer (Thermo Fisher Scientific, USA), respectively.

### Library preparation and sequencing

Libraries were prepared from total RNA by using the NEBNext Ultra II Directional RNA-Seq Kit (NEW ENGLAND BioLabs, UK). Poly(A)-tailed mRNAs were isolated using a Poly(A) RNA Selection Kit (LEXOGEN, Austria). The isolated mRNAs were used for the synthesis of cDNA, which was then sheared, following the manufacturer's instructions. Indexing was performed using the Illumina indices 1-12 (Illumina, USA). The enrichment step was carried out using polymerase chain reaction (PCR). Subsequently, libraries were checked using the Agilent 2100 bioanalyzer (DNA High Sensitivity Kit) to evaluate the mean fragment size. Quantification was performed using the library quantification kit using a StepOne Real-Time PCR System (Life Technologies, USA). High-throughput sequencing (paired-end 100 bp) was performed using HiSeq × 10 (Illumina).

### Data analysis

Quality control of the raw sequencing data was performed using FastQC. Adapter and low-quality reads (<Q20) were removed using FASTX_Trimmer and BBMap. Then the trimmed reads were mapped to the reference genome using TopHat. Gene expression levels were estimated using FPKM (Fragments Per kb per Million reads) values by Cufflinks. The FPKM values were normalized based on the Quantile normalization method using EdgeR within R. Data mining and graphic visualization were performed using ExDEGA (E-biogen, Korea).

### Gene set enrichment analysis (GSEA)

The differential gene expression pattern between asynchronous ESCs and knocked-down mESCs was analyzed using GSEA (ver. 4.1.0) and C5 gene sets, which encompass genes annotated via the same ontology term. The normalized enrichment scores were based on normalized Kolmogorov–Smirnov statistics, and $q$-values were applied to rank the significant pathways enriched in each condition.

### Antibodies
The primary antibodies were rabbit anti-REC8 (ab192241; Abcam, UK), rabbit anti-RAD21 (ab154769; Abcam), rabbit anti-SMC3 (ab9263; Abcam), mouse anti-OCT3/4 (sc5297; Santa Cruz Biotechnology, USA), and rabbit anti–α-tubulin (ab4074; Abcam). The secondary antibodies were AffiniPure goat anti-rabbit IgG (H+L) (111-005-003; Jackson ImmunoResearch, USA) and AffiniPure goat anti-mouse IgG (H+L) (115-005-003; Jackson ImmunoResearch).

### RNA interference
The following commercially available pre-designed small-interfering RNAs (siRNAs) were purchased from Bioneer (Korea) and used to knock down the target genes: *REC8*-specific siRNA (5′-GAGCAAAGAUGUUCUACU-3′), *RAD21*-specific siRNA (5′-GAGUCUUAGGACCUCUGAU-3′), and *SMC3*-specific siRNA (5′-GAGGUUGGCUCAAGCUAC-3′).

Lipofectamine RNAiMAX transfection reagent (13778; Invitrogen, USA) was used to transfect mESCs with the siRNAs. mESCs were seeded in a 60-mm cell culture dish at a density of $2 \times 10^5$ cells and transfected with each siRNA by using Lipofectamine RNAiMAX and Opti-MEM™ Reduced Serum Medium, GlutaMAX™ Supplement (51985034; Gibco) according to the instructions of the manufacturers. AccuTarget™ Negative Control siRNA (SN-1003; Bioneer) was used as a negative control.

### Western blot analysis
Cells were lysed in the cell lysis buffer (50 mM Tris-HCl [pH 7.5], 300 mM NaCl, 0.05% NP40, 5 mM $MgCl_2$, 1 mM DTT, 0.1 mM EDTA, and protease inhibitor cocktail). Lysates (30-50 μg total protein) were electrophoresed on an 8%-10% SDS-polyacrylamide gel, and then the resolved proteins were transferred onto a PVDF (polyvinylidene difluoride) membrane. Membranes were blocked with 5% skim milk in Tris-buffered saline (TBS) with 0.1% Tween 20 and incubated with primary antibodies against REC8 (1:3,000), RAD21 (1:5,000), SMC3 (1:5,000), OCT3/4 (1:3,000), and α-TUBULIN (1:10,000) overnight at 4°C. Membranes were washed with TBS containing 0.1% Tween 20 three times for 10 min and incubated with the secondary antibody for 1 h at 23°C. The membranes were washed three times with TBST (TBS with 0.1% Tween 20) for 10 min each and developed using an ECL system (170-5061; Bio-Rad, USA) according to the manufacturer's directions. Immunoblot detection was conducted using the ChemiDoc MP Imaging system (Bio-Rad).

### Quantitative PCR
Quantitative PCR was used for analyzing the expression levels of the target genes. SYBR Green (K-6251; Bioneer) and the CFX Connect Real-Time PCR system (1855201; Bio-Rad) were used for the experiments. The sequences of the primers used are listed in Supplementary Table S1.

### Statistical analysis
Data were analyzed using the Prism 5 software (GraphPad Software, USA) and are illustrated as mean ± SD. Statistically significant differences between various groups were measured using the Student's *t*-tests. The statistical significance was set at $*P < 0.05$, $**P < 0.01$, and $***P < 0.001$. Each analysis was based on three independent experiments.

### Data availability
The RNA-Seq data were deposited into the NCBI Sequence Read Archive. All the RNA-Seq reads are available under the following accession numbers: SRX10686134 (https://www.ncbi.nlm.nih.gov/sra/?term=SRX10686134), SRX10686135 (https://www.ncbi.nlm.nih.gov/sra/?term=SRX10686135), SRX10686136 (https://www.ncbi.nlm.nih.gov/sra/?term=SRX10686136), and SRX10686137 (https://www.ncbi.nlm.nih.gov/sra/?term=SRX10686137).

## RESULTS

### Reduced expression of cohesin impairs ESC self-renewal
The ultimate role of stem cells is defined in terms of their developmental capacity measured by their differentiation ability (Choi et al., 2020; Zhang and Wang, 2008). The role of cohesin against ESC differentiation has previously been shown (Choi et al., 2022; Khaminets et al., 2020; Noutsou et al., 2017), but whether changes in gene expression are a cause or consequence of promoting ESC self-renewal remains unclear. To define the role of cohesin in regulating ESC differentiation, we depleted the core subunit SMC3 and the kleisin subunit RAD21. We additionally depleted the meiotic cohesin component REC8, which was recently shown to play diverse roles in ESCs (Choi et al., 2022). Depletion of each factor was conducted by treating siRNAs against SMC3, RAD21, and REC8 in ESCs. To investigate the role of cohesin in ESC differentiation, we asked whether knocking down each cohesin subunit promoted ESC differentiation (Fig. 1A). To identify protein expression level, we conducted western blot analysis to examine the knockdown efficiency of cohesin as well as the expression level of OCT3/4, which is commonly used as a stem cell marker. (Fig. 1B). The knockdown efficiency of each cohesin subunit in ESCs was higher than 50%, compared with the subunit levels in the siControl condition (Supplementary Fig. S1A). Additionally, knocking down each cohesin subunit did not influence the expression levels of the other subunits (Supplementary Fig. S1B). Interestingly, relative expression levels of OCT3/4 to GAPDH were drastically decreased in cohesin-knockdown conditions compared with the levels in the control group, meaning that each cohesin subunit, especially RAD21 and SMC3, somehow decreases the level of OCT3/4, raising the possibility that it stimulates the differentiation of ESCs (Fig. 1C; Choi et al., 2022). Further, we investigated quantitative PCR to identify the expression pattern of pluripotency transcription factors OCT3/4, SOX2, KLF4, and NANOG in cohesin-knockdown conditions. As shown in the western blot results, we found decreased expression of the stemness markers in cohesin-knockdown conditions. Whereas every cohesin-knockdown condition showed decreased expression of pluripotency transcription factors, si*RAD21* and si*SMC3* conditions showed a dramatic decrease in each factor compared with the control levels (Fig. 1D). Next, we characterized the morphology of the differentiated cells by using an optical microscope. In contrast to

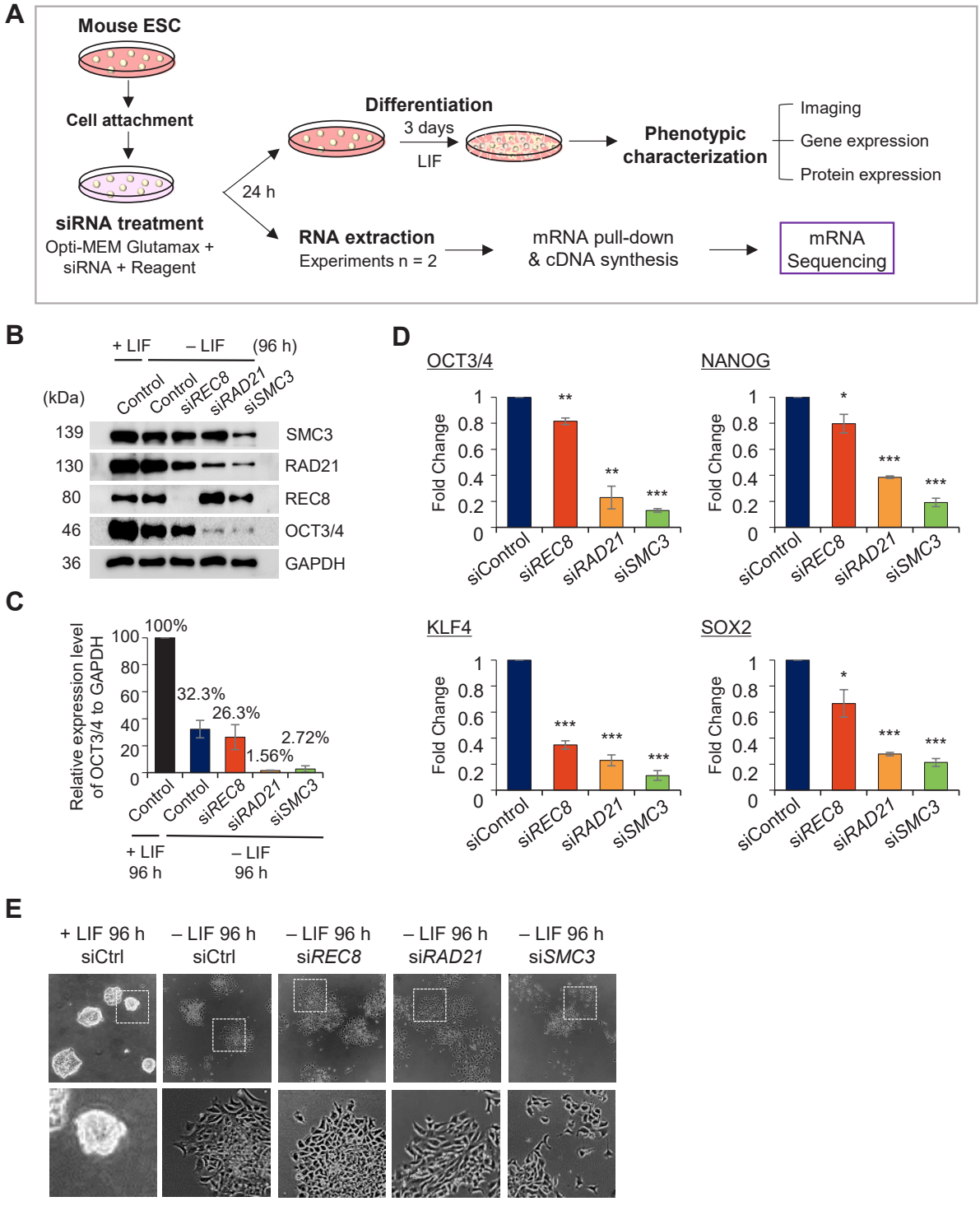


**Fig. 1. Downregulation of cohesin accelerates the differentiation of ESCs.** (A) Schematic overview of the experiment. mESCs were cultured and treated with siControl and cohesin-knockdown siRNAs (si*REC8*, si*RAD21*, and si*SMC3*) for 24 h. RNA was extracted from the cells and mRNA sequencing was conducted. To identify the phenotypic characteristics, cells were differentiated for 96 h. Phenotypes of differentiated cells were identified with microscopy imaging, gene expression pattern, and protein expression pattern. (B and C) Expression analysis of OCT3/4 and cohesin components in cohesin knockdown conditions. Whole-mESC lysates were used. GAPDH was used as a loading control. Three independent experiments were conducted to analyze the data. (D) Expression analysis of stemness markers using quantitative PCR. Results are illustrated as the mean ± SD values from three independent experiments. *P*-values were calculated by paired *t*-test using GraphPad Prism 5 software (**P* < 0.05; ***P* < 0.001; ****P* < 0.0001). (E) Microscopy imaging of differentiated ESC in each condition (Control, si*REC8*, si*RAD21*, si*SMC3*). Cells were cultured and differentiated for 96 h in each condition.

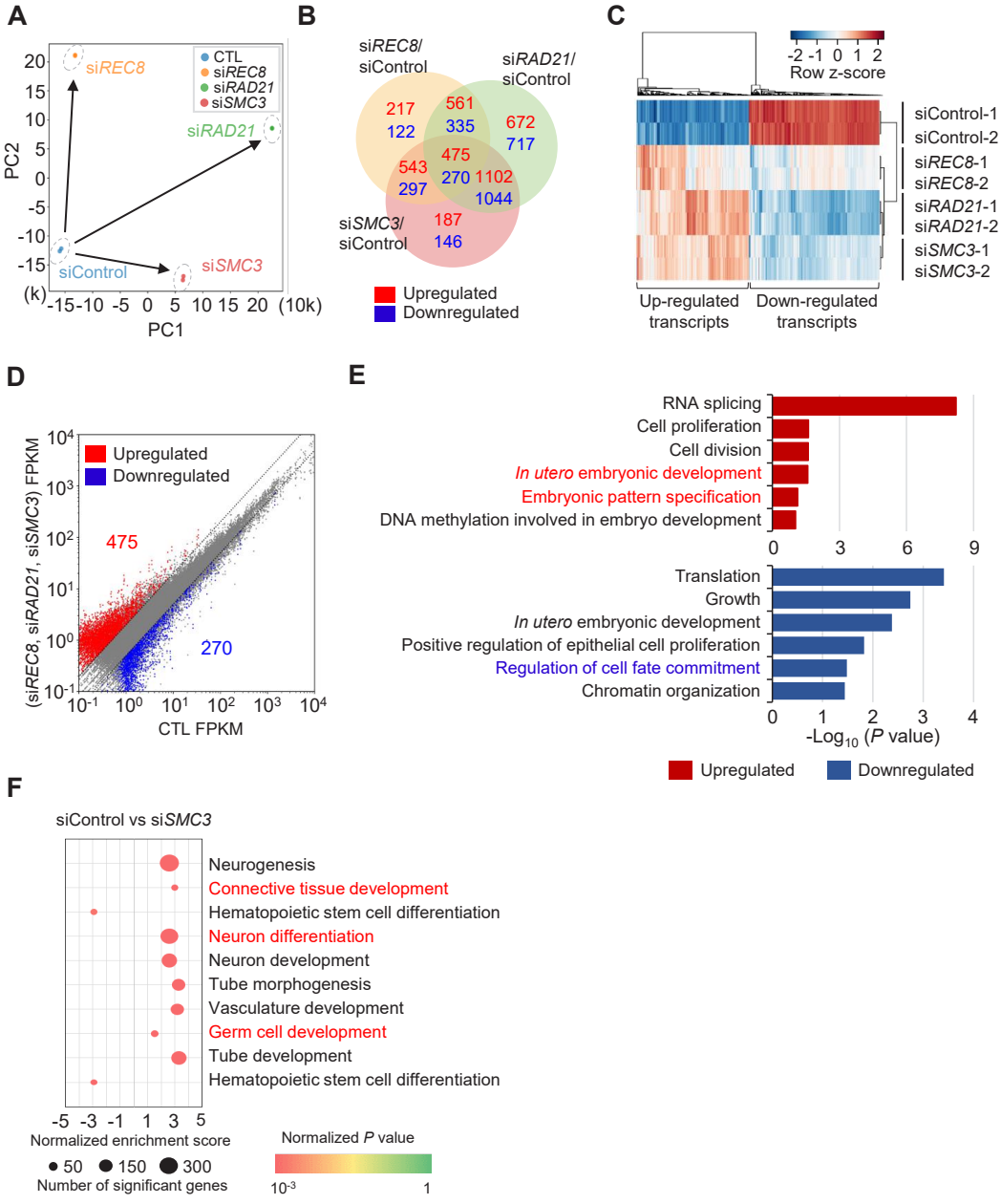


**Fig. 2. Gene expression profile of ESCs upon knocking down cohesin.** (A) PCA plot of experimental sets. For mRNA sequencing, two independent experiments were performed. The clustering pattern was confirmed by the PCA plot. PC1 and PC2 stand for two principal components respectively. The values indicate the amount of variation that attributes to each principal component. All the samples were biologically duplicated (n = 2). PCA, principal component analysis; CTL, control. (B) Venn diagram of differentially expressed genes (DEGs) from siRNA-mediated knockdown of REC8, RAD21, and SMC3 in ESCs (FPKM > 1, fold change > 1.5, *P* value < 0.01). Red: upregulation with FPKM > 1, |fold change| > 1.5, *P* value < 0.01; Blue: downregulation with FPKM > 1, |fold change| > 1.5, *P* value < 0.01. (C) A hierarchical clustering heatmap illustrating DEGs in cohesin-knockdown conditions (FPKM > 1, fold change > 1.5, *P* value < 0.01). Rows of DEGs and columns of each condition were both clustered, respectively. Mapping grids are colored according to their row z-scores. (D) Volcano plot of 475 upregulated genes and 270 downregulated genes. Three volcano plots of cohesin-knockdown/siControl condition were overlapped in one plot, and commonly regulated gene sets are indicated with colors. Red: upregulation with FPKM > 1, |fold change| > 1.5, *P* value < 0.01; Blue: downregulation with FPKM > 1, |fold change| > 1.5, *P* value < 0.01. (E) Analyses of the DEGs were performed by using the DAVID database. Enriched biological themes, especially gene ontology terms were identified in both upregulated and downregulated genes. The upper red plot indicates GO terms enriched in upregulated genes; the blue plot shows GO terms enriched in downregulated genes. *P* values in x-axis are illustrated in $-\text{Log}_{10}$ (*P* value). (F) GSEA analysis for DEGs in SMC3 knockdown condition (fold change ≥ 1.3, fold change ≤ 0.8). GSEA was analyzed with mRNA-seq data from two independent experiments. Normalized *P* values were used to adjust the data. The cut-off value to reject the null hypothesis was set at 0.05, which means the extreme value for the test statistic is expected <5% of the time.

the normal dome-shaped colony morphology, cells cultured without LIF showed a differentiated morphology, exhibiting a mechanically stretched, flat colony morphology. Meanwhile, we observed that the ESCs in the cohesin-knockdown conditions were far more spread than the control cells and showed approximately 12-h faster differentiation (Fig. 1E).

### Cohesin regulates the expression of genes involved in cell-fate determination

Several studies have suggested the role of cohesin in changing chromatin architecture, especially those of key self-renewal–related genes (Haering and Jessberger, 2012; Kagey et al., 2010; Noutsou et al.,2017; Sofueva et al., 2013). As the knockdown of each cohesin subunit promoted ESC differentiation, mRNA sequencing (RNA-seq) was performed to verify the differences in global gene expression patterns between the control and cohesin-knockdown groups. To minimize the possibility of misinterpretations, we analyzed RNA-seq data from two independent experiments. PCA (principal component analysis) was used to interpret the suitability of the two independent experiments as biological replicates, as well as the association between each sample (Fig. 2A). The similarity between the two independent groups was high enough to use them as biological replicates, and each group showed distinct distances between one another, meaning that each group has a different gene expression pattern (Supplementary Fig. S2). For further study, a Venn diagram displaying the upregulated and downregulated transcripts was generated based on the normalized data with FPKM > 1, fold change > 1.5, and *P* value < 0.01 (Fig. 2B). Genes listed via hierarchical clustering revealed that each cohesin-subunit knockdown condition showed a completely different pattern of gene expression compared with that of the control group (Fig. 2C). To understand the general characteristics of cohesin, commonly upregulated and downregulated genes were visualized in a volcano plot (Fig. 2D). "Database for annotation, visualization, and integrated discovery" (DAVID) bioinformatics resources were used to identify enriched biological GO (Gene Ontology) terms of 475 commonly upregulated genes and 270 commonly downregulated genes. The GO terms for the upregulated genes were as follows: DNA methylation involved in embryo development, embryonic pattern specification, *in utero* embryonic development, cell division, cell proliferation, and RNA splicing. Additionally, the following GO terms corresponded to the downregulated genes: chromatin organization, regulation of cell fate commitment, positive regulation of epithelial cell proliferation, *in utero* embryonic development, growth, and translation (Fig. 2E). These data showed that the genes that were commonly regulated were closely related to cell differentiation.

### mESCs with si*REC8* exhibit a different pattern of differentiation than mESCs with si*RAD21*

The correlation of cohesin with differentiation has been studied by several groups (Galeev et al., 2016; Khaminets et al., 2020; Viny et al., 2019), yet the role of cohesin in controlling ESC differentiation has not been elucidated. As we identified the fact that cohesin regulates the differentiation pattern, we decided to assess the genes whose expression was differentially regulated in each cohesin subunit knockdown condition. To investigate the differentiation pattern in the context of cohesin loss, we decided to analyze the genes whose expression levels are differentially regulated in the si*SMC3* condition, in which the core subunit of cohesin is depleted. GSEA revealed that upregulated and downregulated genes (fold change above 1.3, below 0.8) in si*SMC3* condition exhibit lineage-controlled differentiation to connective tissue, neuron, and germ cell (Fig. 2F). We hypothesized that depletion of each cohesin subunit not only induces alteration in translational output, which results in a different pattern of differentiation but also regulates the fate of ESCs (i.e., differentiation to a specific lineage). As SMC3 is the core subunit of cohesin, we wondered whether the kleisin subunits of cohesin induce differentiation to a specific lineage and decided to assess the genes whose expression levels are co-regulated in the si*REC8* and si*RAD21* conditions (fold change > 1.5, *P* value < 0.05) (Supplementary Fig. S3A). To our surprise, we found out that the genes commonly upregulated were enriched in the biological term "cell differentiation" (Supplementary Figs. S3B and S3C). We decided to compare the si*REC8* and si*RAD21* as they might regulate more specifically lineage of differentiation. In this regard, a Venn diagram of the si*REC8* and si*RAD21* conditions was generated (Fig. 3A). The *REC8*-depleted condition showed 205 and 260 significantly upregulated and downregulated genes, respectively, compared with the expression levels in the si*RAD21* condition. GSEA revealed that REC8-deficient ESCs showed positive enrichment of genes associated with the developmental processes and anatomical structure formation involved in morphogenesis (Fig. 3B). Given that the commonly regulated genes in the cohesin-reduced condition showed meaningful fluctuation in the translational process, the protein modification process was highly regulated upon *REC8* knockdown. Interestingly, the developmental processes related to the circulatory system showed a higher enrichment score than the control group.

To identify if REC8 knockdown induces circulatory system development, we classified five related GO terms to understand the gene expression pattern of each group. The five terms are as follows: positive regulation of cell differentiation, anatomical structure formation involved in morphogenesis, blood vessel morphogenesis, vasculature development, and circulatory system development. The set-to-set analysis was performed to understand the correlation among the five groups. "Blood vessel morphogenesis," "vasculature development," and "circulatory system development" showed high intensity, as these terms could be grouped by the term "angiogenesis." Intriguingly, the genes enriched in the term "anatomical structure formation involved in morphogenesis" showed a strong correlation with angiogenesis-related groups, as mentioned above. Indeed, a heatmap of leading-edge genes in each group revealed a fair number of genes co-regulated in each group (Fig. 3D). Meanwhile, groups of genes in positive regulation of cell differentiation with other groups showed a lower intensity of interaction, showing a relatively less overlap among the leading-edge genes (Fig. 3C). To test which genes are in charge of regulating lineage-specific differentiation, a heatmap of leading-edge genes in each group was generated (Fig. 3D). Above all, the *Ccn1* gene, which is recently re-

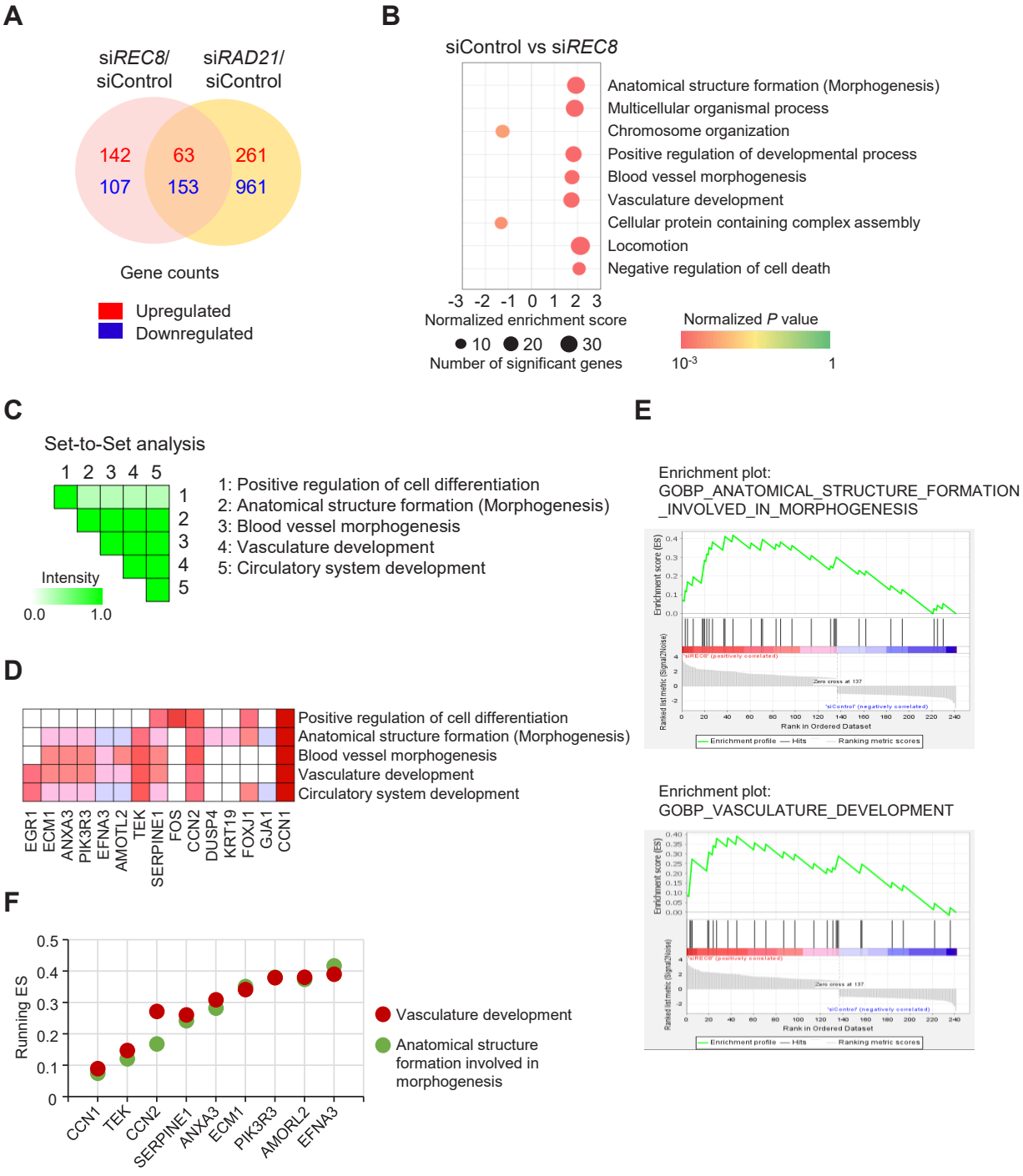


**Fig. 3. Distribution of differentially expressed genes (DEGs) in ESC following knockdown of REC8.** (A) Venn diagram of all unique and common DEGs in si*REC8*/siControl and si*RAD21*/siControl (fold change > 1.5, *P* value < 0.01). (B) GSEA analysis for DEGs in REC8 knockdown condition. GSEA was analyzed with mRNA-seq data from two independent experiments. To adjust the data, we used the normalized *P* value. The cut-off value to reject the null hypothesis was set at 0.05, which means the extreme value for the test statistic is expected <5% of the time. (C) Set-to-set analysis showing the correlation among the GO terms. The intensity was measured by the number of genes that are co-regulated in two GO terms. Higher intensity indicates there are larger overlapping genes. (D) Heatmap of leading-edge genes in each GO term. Expression values are represented as colors, where the range of colors (red, pink, light blue, and dark blue) shows the range of expression values (high, moderate, low, and lowest, respectively). (E) Enrichment plot generated by GSEA. Anatomical structure formation involved in morphogenesis and vasculature development associated gene sets were highly enriched in si*REC8* condition. (F) Dot plot comparing running enrichment score for the gene set. Genes that are overlapped in two gene ontology terms (anatomical structure formation involved in morphogenesis, vasculature development) are indicated in the plot.

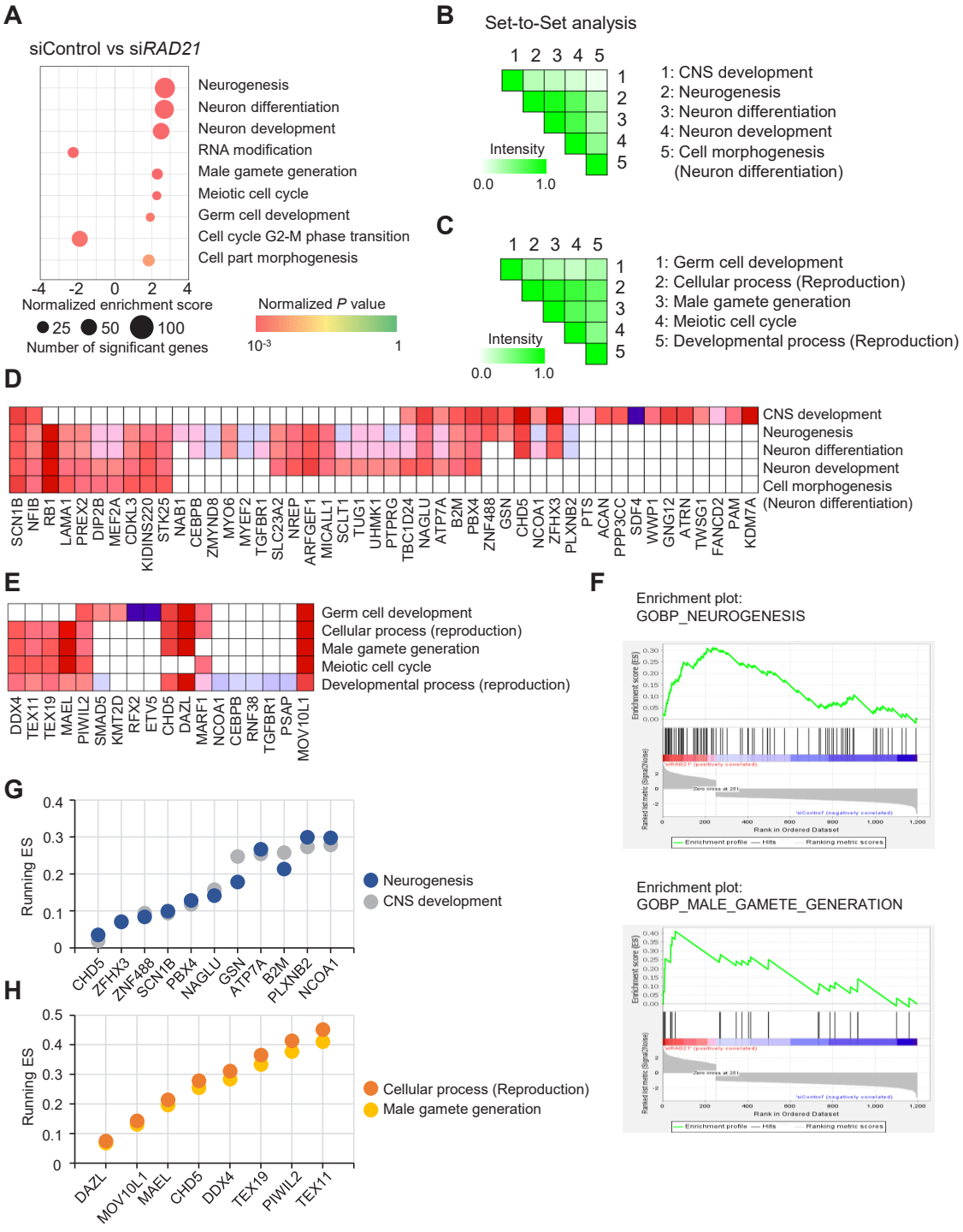


**Fig. 4. Distribution of differentially expressed genes (DEGs) in ESC following knockdown of RAD21.** (A) GSEA analysis for DEGs in the RAD21 knockdown condition. GSEA was analyzed with mRNA-seq data from two independent experiments. To adjust the data, we used the normalized *P* value. The cut-off value to reject the null hypothesis was set at 0.05, which means that the extreme value for the test statistic is expected to be <5% of the time. (B and C) Set-to-set analysis showing a correlation between GO terms. The intensity was measured by the number of genes that are co-regulated in two GO terms. Higher intensity indicates there are larger overlapping genes. (D and E) Heatmap of leading-edge genes in each GO term. Expression values are represented as colors, where the range of colors (red, pink, light blue, and dark blue) shows the range of expression values (high, moderate, low, and lowest, respectively). (F) Enrichment plot generated by GSEA. Neurogenesis and male gamete generation-associated gene sets were highly enriched in the si*RAD21* condition. (G and H) Dot plot comparing running enrichment scores for the gene set. Genes that are overlapped in two gene ontology terms (neurogenesis and CNS development, and cellular processes involved in reproduction and spermatogenesis) are indicated in the plot.

vealed to regulate endothelial tip cell activity in angiogenesis (Park et al., 2019), showed a high enrichment score in every GO term. Other genes that are enriched in five terms may also contribute to angiogenesis. GSEA results showed *Ccn2*, CTGF (connective tissue growth factor), which promotes the differentiation and proliferation of vascular endothelial cells (Takigawa, 2013), and *Serpine1*, a key regulator of angiogenesis, which is reported to induce tumor vascularization (Li et al., 2018; Xu et al., 2019).

As each GO term contains redundant overlapping genes, we analyzed each GO term and chose two terms that represent functional attributes of the si*REC8* group; anatomical structure formation involved in morphogenesis and vasculature development (Fig. 3E). To identify the relative enrichment score of co-regulated genes, we compared the running enrichment score, which indicates the enrichment score at the point in the ranked list of genes. As shown in Fig. 3F, six out of the nine genes had higher running enrichment score (ES) in vascular development (Fig. 3F). Taken together, our result shows that the gene sets involved in vasculature development (i.e., angiogenesis) are markedly enriched in the si*REC8* condition. However, the si*RAD21* gene set showed a distinctive differentiation pattern from the si*REC8* gene set. GSEA analysis using the 261 upregulated genes and 961 downregulated genes revealed that genes involved in neurogenesis (neuron differentiation and development) and gametogenesis (meiotic cell cycle and germ cell development) were highly represented in si*RAD21* cells compared with the levels in the siControl cells (Fig. 4A). Set-to-set analysis showed that neurogenesis, neuron differentiation, and neuron development showed a high correlation with each group. The cell morphogenesis involved in neuron differentiation and CNS development was not highly correlated with other terms; nevertheless, there were several commonly regulated genes (Fig. 4B). In the case of gametogenesis-related terms, the cellular processes involved in reproduction showed high intensity with other terms, indicating there are huge overlaps with other groups. Meanwhile, genes that are involved in germ cell development showed lower intensity when compared with other groups (Fig. 4C). Heatmaps generated with leading-edge genes of each group showed that *Scn1b*, which is known for its role in the generation and propagation of action potential in muscle and neuronal cells (Patino et al., 2009), was highly enriched in GO terms that were related with neuron differentiation. *Nfib*, which is necessary for neural stem and progenitor cell differentiation (Betancourt et al., 2014), also showed high enriched status in every GO term (Fig. 4D). Furthermore, *Mov10l1* and *Piwil2* showed high enrichment scores in every GO term related to gametogenesis, showing that these two genes, especially *Mov10l1*, may function as a key regulator in the germ cell developmental processes (Fig. 4E). Specifically expressed in germ cells, *Mov10l1* functions as a key component of maintaining genetic information in male germ cells of mammals (Frost et al., 2010). We chose two ranking metrics in GSEA that are thought to be the main characteristic of the si*RAD21* group. Results of GSEA showed neurogenesis and CNS development; cellular process involved in reproduction and male gamete generation (Fig. 4F). Six out of 11 co-regulated genes showed a higher running ES in neurogenesis, indicating that more than half of the co-regulated genes have a more significant effect on neurogenesis (Fig. 4G). Given that the DEGs (differentially expressed genes) in the si*RAD21* group were largely involved in neurogenesis, our data indicate that the gene set involved in neurogenesis was highly enriched in the si*RAD21* condition. Additionally, the gene sets that were co-regulated in the two GO terms, (i.e., the cellular process involved in reproduction and male gamete generation) revealed that every gene showed a higher running enrichment score in the cellular process involved in reproduction. As the gene set involved in the germ cell development was too small to interpret compared with the neurogenesis-related genes, we tentatively concluded that si*RAD21* influenced not only spermatogenesis but is also more likely to be involved in the overall cellular process involved in reproduction (Fig. 4H).

## Mitotic cohesin RAD21 regulates lineage differentiation of mESCs

Although ESC is characterized by pluripotency and self-renewal, our result reveals that knocking down cohesin in ESC induces lineage-specific differentiation *in vitro*. To analyze the effect of cohesin knockdown in lineage-specific differentiation, we used the DAVID tool to find out how genes related to differentiation are regulated under those conditions. The enriched annotation terms identified by DAVID in each cohesin knockdown group were spermatogenesis (GO: 0007283) and nervous system development (GO: 0007399) in si*RAD21* (Fig. 5A). Those terms identified by DAVID showed that the biological theme underlying cell differentiation in the cohesin-knockdown condition was cell-type-specific differentiation. For further analysis, we aimed to verify our hypothesis about the role of cohesin in controlling the lineage-specific differentiation in ESCs. Since differentiated cells exhibit specific genes that produce the proteins characteristic for each type of cell, we decided to use lineage markers to determine whether the cohesin-knockdown condition regulates the lineage specification of differentiation or not. As such, we quantified the *in vitro* lineage-specific differentiation capacity of cohesin-knockdown condition mESC relative to the control condition at the level of cellular differentiation (Fig. 5B). Given that RNA sequencing data showed a tendency of differentiation to the specific cell type, we analyzed data with previously reported lineage markers of each cell type: NES and NEUROD1 for neural lineage markers (Gao et al., 2009; Suzuki et al., 2010) and STRA8 and DDX4 for germline lineage markers (Ma et al., 2018; Nicholls et al., 2019; Poon et al., 2016). Based on the mRNA sequencing data, we analyzed the expression level of each lineage marker by using the average of normalized data ($Log_2$ [raw sequencing read]). Given that the RNA-seq data were generated by using undifferentiated mESCs, elevated levels of lineage markers underpin the lineage-specific differentiation potential of ESC in the cohesin-knockdown condition (Fig. 5B).

ESCs in each cohesin subunit knockdown condition were further differentiated to characterize the identity of final differentiated cell populations. For this analysis, we used real-time PCR to determine whether differentiated cells in the cohesin-knockdown conditions express lineage-specific mark-

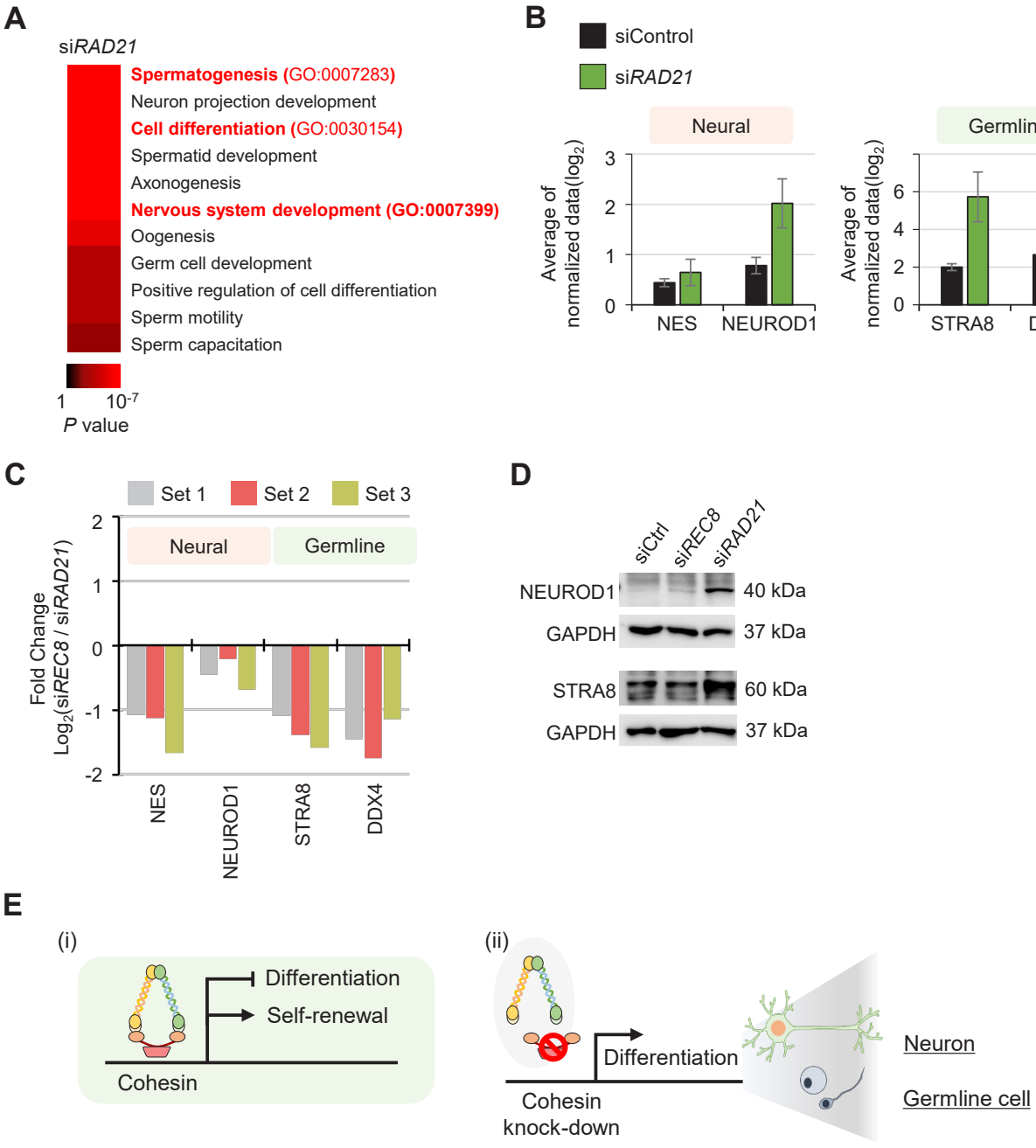


**Fig. 5. Cell-type-specific differentiation upon knocking down cohesin.** (A) Enriched annotations of differentiation-related genes (GO: 0007399) in the si*RAD21* condition. DAVID was used to interpret biological themes, especially gene ontology terms that are enriched in each condition. P-values are illustrated in color. (B) Bar graphs showing the expression levels of lineage-specific markers. Two genes were selected as representative markers of each of the endothelium, neural, and germline lineages (Endothelium lineage markers: ENG, GATA4; Neural lineage markers: NES, NEUROD1; Germline lineage markers: STRA8, DDX4). Y-axis indicates the average of normalized data ($log_2$). (C) Expression analysis of lineage-specific markers using quantitative PCR. Three independent sets of cDNA were used for quantitative PCR, and fold changes of si*REC8* to si*RAD21* were normalized using the $log_2$ value. (D) Expression analysis of lineage-specific markers using western blot analysis. (E) Lineage-specific differentiation induced by cohesin depletion. Proposed model of lineage-specific differentiation in cohesin knockdown conditions. Reduced expression of cohesin impairs self-renewal, and the knockdown of each cohesin subunit in mESCs is positioned to different fate developments.

ers. Neural and germline lineage markers turned out to be highly expressed in differentiated cells of the si*RAD21* condition compared with the differentiated cells of the si*REC8* condition. Neural marker NES and NEUROD1 exhibited 2.46-fold and 1.37-fold higher expression levels, respectively, in the si*RAD21* condition compared with the si*REC8* condition

(Fig. 5C). Additionally, the si*RAD21* condition also showed increased expression levels of germline lineage markers, 2.57-fold in STRA8 and 2.74-fold in DDX4 (Fig. 5C). Further, the reference genes *NEUROD1* and *STRA8* were found upregulated based on western blotting analyses (Fig. 5D). These data suggest that ESCs with si*RAD21* are biased to differentiate into neural and germline cells. Collectively, our study demonstrates that each cohesin subunit RAD21 not only supports ESCs pluripotency but also controls ESC fate determination.

## DISCUSSION

Since the development of the methods that control the differentiation of ESCs into specific lineages is of interest, the field of stem cell research has been the center of attention given the ability of ESCs to differentiate into every somatic cell type in the embryo proper. With the expectation of serving as an everlasting cell source to generate functional cells, the harnessing of ESCs is considered a promising therapeutic strategy to treat diverse human diseases. Therefore, several studies are being done to improve the effectiveness of differentiation of ESCs into specific cell types (Gamage et al., 2016; Potter et al., 2014; Willerth et al., 2006). The major limitations of this strategy are that the properties of ESCs and differentiated cells are not described in detail (Choumerianou et al., 2008; Steinbeck and Studer, 2015).

The cohesin complex is a multi-functional complex that exerts various biological processes ranging from organizing chromosome dynamics to controlling self-renewal activity and differentiation of ESCs. Several studies have described the correlation between cohesin and cell differentiation (Mazzola et al., 2019; Sasca et al., 2019), but its exact role in regulating ESC differentiation remains unclear. Through functional analysis of cohesin knockdown conditions, our findings suggest the novel role of cohesin that may function to maintain the balance of self-renewal and differentiation. By using four transcriptional factors that are known to be essential for maintaining the pluripotency of ESCs—Oct4 (Pou5f1), Nanog, Sox2, and Klf4 (Han et al., 2021; Takahashi and Yamanaka et al., 2006)—we aimed to identify the role of cohesin in the pluripotency of ESCs. Knockdown of each cohesin subunit showed decreased expression of pluripotency markers, but among them, si*RAD21* and si*SMC3* conditions showed a dramatic decrease in the expression of every marker (Figs. 1B-1D). For further study, we observed the differentiation pattern of each condition. Reduced expression of each cohesin subunit promoted ESCs differentiation, showing differentiated form in 24 h after siRNA treatment (data not shown). The reduced expression of stemness markers and rapid ESC differentiation in cohesin-knockdown conditions implied that reduced expression of cohesin attenuates the dissolution of pluripotency.

As the role of cohesin in regulating self-renewal genes has been reported by several researchers, our identification has its further focus on the detailed networks between reduced expression of cohesin and the pattern of differentiation. Using RNA-seq, we performed the first transcriptomic analysis of ESCs in the cohesin-knockdown conditions and observed a significant association between each cohesin subunit knockdown and differentiation to a specific cell type. To address the global gene expression pattern, we identified the genes that were co-regulated in the cohesin-knockdown condition using the DAVID tool. DAVID analysis showed that genes that are up- or down-regulated showed highly enriched biological terms related to differentiation. As SMC3 is the core subunit of cohesin, we decided to analyze the si*SMC3* condition to define the detailed biological terms that are enriched in the cohesin-knockdown condition. Intriguingly, GSEA analysis revealed that knocking down the SMC3 subunit resulted in lineage-specific differentiation, which was classified into three lineages: connective tissue development, neuron differentiation, and germ cell development. We hypothesized that depletion of each cohesin subunit not only induces alteration in the translational output that results in ESC differentiation but also regulates the fate of ESCs (i.e., differentiation to a specific lineage). In the context that si*REC8* or si*RAD21* condition may regulate more specific lineage of differentiation, we compared two conditions to understand which biological terms are enriched in those conditions. In the si*REC8* condition, genes that regulate differentiation into endothelial cells were upregulated, and in the si*RAD21* condition, genes that regulate differentiation into either neural or germ cells were upregulated. Among the GO terms that are enriched in each condition, the si*REC8* condition exhibited a strong running enrichment score in vasculature development, and the si*RAD21* condition showed a high enrichment score in the neurogenesis and cellular processes involved in reproduction.

Since differentiated cells exhibit specific genes that produce the proteins characteristic for each type of cell, we decided to use lineage markers to determine whether the cohesin-knockdown conditions regulate the lineage specification of differentiation or not. By using two markers for each lineage, we identified the expression levels of lineage-specific markers by comparing RNA-sequencing data of undifferentiated cells and quantitative PCR data of differentiated cells. The RNA-sequencing data revealed that except for the endothelium lineage marker GATA4, which showed a slight downregulation in the si*REC8* condition (0.95-fold compared with the level siControl condition), the cohesin-knockdown conditions showed elevated expression in every lineage-specific marker. Additionally, differentiated cells in each cohesin-knockdown condition showed elevated levels of each lineage-specific factor, which indicates differentiation into neural or germline lineage cells in the si*RAD21* condition (Fig. 5E). However, there is a possibility that differentiation characteristics may appear differently due to differential expression levels of cohesin subunits.

Taken together, our results indicate that these networks significantly contribute to the lineage differentiation of ESCs which is considered a major challenge for the clinical application of stem cells. While we cannot ignore the constraints of any unrevealed signaling pathway and its applicability *in vivo*, our study has significance in that it provides evidence that signaling induced by cohesin is likely to play an essential role in finding efficient ways to guide lineage commitment.

*Note: Supplementary information is available on the Mole-*

*cules and Cells website (www.molcells.org).*

## ACKNOWLEDGMENTS

This work was supported by grants from the National Research Foundation of Korea, funded by the Ministry of Science, ICT & Future Planning (No. 2020R1A2C2011887; 2018R1D1A1B07050755), the Korea Environment Industry & Technology Institute through "Digital Infrastructure Building Project for Monitoring, Surveying and Evaluating the Environmental Health Program (No. 2021003330007)" funded by Korea Ministry of Environment, and the BioGreen 21 Program (No. PJ015708) funded by Rural Development Administration, Republic of Korea.

## AUTHOR CONTRIBUTIONS

Y.E.K. performed the experiments. Y.E.K., E.H.C., J.W.K., and K.P.K. analyzed the data. K.P.K. conceived and supervised the study. All authors wrote and edited the manuscript.

## CONFLICT OF INTEREST

The authors have no potential conflicts of interest to disclose.

## ORCID

| | |
|---|---|
| Young Eun Koh | https://orcid.org/0000-0002-9116-2384 |
| Eui-Hwan Choi | https://orcid.org/0000-0003-1547-2580 |
| Jung-Woong Kim | https://orcid.org/0000-0003-4458-7213 |
| Keun Pil Kim | https://orcid.org/0000-0002-5973-8259 |

## REFERENCES

Betancourt, J., Katzman, S., and Chen, B. (2014). Nuclear factor one B regulates neural stem cell differentiation and axonal projection of corticofugal neurons. J. Comp. Neurol. *522*, 6-35.

Biswas, U., Hempel, K., Llano, E., Pendas, A., and Jessberger, R. (2016). Distinct roles of meiosis-specific cohesin complexes in mammalian spermatogenesis. PLoS Genet. *12*, e1006389.

Brooker, A.S. and Berkowitz, K.M. (2014). The roles of cohesins in mitosis, meiosis, and human health and disease. Methods Mol. Biol. *1170*, 229-266.

Choi, E.H., Yoon, S., Hahn, Y., and Kim, K.P. (2017). Cellular dynamics of Rad51 and Rad54 in response to postreplicative stress and DNA damage in HeLa cells. Mol. Cells, *40*, 143-150.

Choi, E.H., Yoon, S., Koh, Y.E., Hong, T.K., Do, J.T., Lee, B.K., Hahn, Y., and Kim, K.P. (2022). Meiosis-specific cohesin complexes display essential and distinct roles in mitotic embryonic stem cell chromosomes. Genome Biol. *23*, 70.

Choi, E.H., Yoon, S., Koh, Y.E., Seo, Y.J., and Kim, K.P. (2020). Maintenance of genome integrity and active homologous recombination in embryonic stem cells. Exp. Mol. Med. *52*, 1220-1229.

Choumerianou, D.M., Dimitriou, H., and Kalmanti, M. (2008). Stem cells: promises versus limitations. Tissue Eng. Part B Rev. *14*, 53-60.

Cuartero, S., Weiss, F.D., Dharmalingam, G., Guo, Y., Ing-Simmons, E., Masella, S., Robles-Rebollo, I., Xiao, X., Wang, Y.F., Barozzi, I., et al. (2018). Control of inducible gene expression links cohesin to hematopoietic progenitor self-renewal and differentiation. Nat. Immunol. *19*, 932-941.

Efthymiou, A.G., Chen, G., Rao, M., Chen, G., and Boehm, M. (2014). Self-renewal and cell lineage differentiation strategies in human embryonic stem cells and induced pluripotent stem cells. Expert Opin. Biol. Ther. *14*, 1333-1344.

Findikli, N., Candan, N.Z., and Kahraman, S. (2006). Human embryonic stem cell culture: current limitations and novel strategies. Reprod. Biomed. Online *13*, 581-590.

Frost, R.J., Hamra, F.K., Richardson, J.A., Qi, X., Bassel-Duby, R., and Olson, E.N. (2010). MOV10L1 is necessary for protection of spermatocytes against retrotransposons by Piwi-interacting RNAs. Proc. Natl. Acad. Sci. U. S. A. *107*, 11847-11852.

Galeev, R., Baudet, A., Kumar, P., Rundberg Nilsson, A., Nilsson, B., Soneji, S., Törngren, T., Borg, Å., Kvist, A., and Larsson, J. (2016). Genome-wide RNAi screen identifies cohesin genes as modifiers of renewal and differentiation in human HSCs. Cell Rep. *14*, 2988-3000.

Gamage, T.K., Chamley, L.W., and James, J.L. (2016). Stem cell insights into human trophoblast lineage differentiation. Hum. Reprod. Update *23*, 77-103.

Gao, Z., Ure, K., Ables, J.L., Lagace, D.C., Nave, K.A., Goebbels, S., Eisch, A.J., and Hsieh, J. (2009). Neurod1 is essential for the survival and maturation of adult-born neurons. Nat. Neurosci. *12*, 1090-1092.

Gorecka, J., Kostiuk, V., Fereydooni, A., Gonzalez, L., Luo, J., Dash, B., Isaji, T., Ono, S., Liu, S., Lee, S.R., et al. (2019). The potential and limitations of induced pluripotent stem cells to achieve wound healing. Stem Cell Res. Ther. *10*, 87.

Haering, C.H. and Jessberger, R. (2012). Cohesin in determining chromosome architecture. Exp. Cell Res. *318*, 1386-1393.

Han, S., Lee, H., Lee, A.J., Kim, S., Jung, I., Koh, G.Y., Kim, T., and Lee, D. (2021). CHD4 conceals aberrant CTCF-Binding sites at TAD interiors by regulating chromatin accessibility in mouse embryonic stem cells. Mol. Cells *44*, 805-829.

Heng, B.C., Cao, T., and Lee, E.H. (2004). Directing stem cell differentiation into the chondrogenic lineage in vitro. Stem Cells *22*, 1152-1167.

Hirano, T. (2015). Chromosome dynamics during mitosis. Cold Spring Harb. Perspect. Biol. *7*, a015792.

Hong, S., Joo, J.H., Yun, H., and Kim, K. (2019). The nature of meiotic chromosome dynamics and recombination in budding yeast. J. Microbiol. *57*, 221-231.

Ishiguro, K. (2019). The cohesin complex in mammalian meiosis. Genes Cells *24*, 6-30.

Kagey, M.H., Newman, J.J., Bilodeau, S., Zhan, Y., Orlando, D.A., van Berkum, N.L., Ebmeier, C.C., Goossens, J., Rahl, P.B., Levine, S.S., et al. (2010). Mediator and cohesin connect gene expression and chromatin architecture. Nature *467*, 430-435.

Keller, G. (2005). Embryonic stem cell differentiation: emergence of a new era in biology and medicine. Genes Dev. *19*, 1129-1155.

Khaminets, A., Ronnen-Oron, T., Baldauf, M., Meier, E., and Jasper, H. (2020). Cohesin controls intestinal stem cell identity by maintaining association of Escargot with target promoters. Elife *9*, e48160.

Li, S., Wei, X., He, J., Tian, X., Yuan, S., and Sun, L. (2018). Plasminogen activator inhibitor-1 in cancer research. Biomed. Pharmacother. *105*, 83-94.

Ma, H.T., Niu, C.M., Xia, J., Shen, X.Y., Xia, M.M., Hu, Y.Q., and Zheng, Y. (2018). Stimulated by retinoic acid gene 8 (Stra8) plays important roles in many stages of spermatogenesis. Asian J. Androl. *20*, 479-487.

Mazzola, M., Deflorian, G., Pezzotta, A., Ferrari, L., Fazio, G., Bresciani, E., Saitta, C., Ferrari, L., Fumagalli, M., Parma, M., et al. (2019). NIPBL: a new player in myeloid cell differentiation. Haematologica *104*, 1332-1341.

Mehta, G.D., Rizvi, S.M., and Ghosh, S.K. (2012). Cohesin: a guardian of genome integrity. Biochim. Biophys. Acta *1823*, 1324-1342.

Murry, C.E. and Keller, G. (2008). Differentiation of embryonic stem cells to clinically relevant populations: lessons from embryonic development. Cell *132*, 661-680.

Nasmyth, K. and Haering, C.H. (2009). Cohesin: its roles and mechanisms. Annu. Rev. Genet. *43*, 525-558.

Nicholls, P.K., Schorle, H., Naqvi, S., Hu, Y.C., Fan, Y., Carmell, M.A., Dobrinski, I., Watson, A.L., Carlson, D.F., Fahrenkrug, S.C., et al. (2019). Mammalian germ cells are determined after PGC colonization of the nascent gonad. Proc. Natl. Acad. Sci. U. S. A. *116*, 25677-25687.

Noutsou, M., Li, J., Ling, J., Jones, J., Wang, Y., Chen, Y., and Sen, G.L. (2017). The cohesin complex is necessary for epidermal progenitor cell function through maintenance of self-renewal genes. Cell Rep. *20*, 3005-3013.

Park, M.H., Kim, A.K., Manandhar, S., Oh, S.Y., Jang, G.H., Kang, L., Lee, D.W., Hyeon, D.Y., Lee, S.H., Lee, H.E., et al. (2019). CCN1 interlinks integrin and hippo pathway to autoregulate tip cell activity. Elife *8*, e46012.

Patino, G.A., Claes, L.R., Lopez-Santiago, L.F., Slat, E.A., Dondeti, R.S., Chen, C., O'Malley, H.A., Gray, C.B., Miyazaki, H., Nukina, N., et al. (2009). A functional null mutation of SCN1B in a patient with Dravet syndrome. J. Neurosci. *29*, 10764-10778.

Peters, J.M., Tedeschi, A., and Schmitz, J. (2008). The cohesin complex and its roles in chromosome biology. Genes Dev. *22*, 3089-3114.

Poon, J., Wessel, G.M., and Yajima, M. (2016). An unregulated regulator: Vasa expression in the development of somatic cells and in tumorigenesis. Dev. Biol. *415*, 24-32.

Potter, C.M., Lao, K.H., Zeng, L., and Xu, Q. (2014). Role of biomechanical forces in stem cell vascular lineage differentiation. Arterioscler. Thromb. Vasc. Biol. *34*, 2184-2190.

Revenkova, E., Eijpe, M., Heyting, C., Hodges, C.A., Hunt, P.A., Liebe, B., Scherthan, H., and Jessberger, R. (2004). Cohesin SMC1 beta is required for meiotic chromosome dynamics, sister chromatid cohesion and DNA recombination. Nat. Cell Biol. *6*, 555-562.

Sasca, D., Yun, H., Giotopoulos, G., Szybinski, J., Evan, T., Wilson, N.K., Gerstung, M., Gallipoli, P., Green, A.R., Hills, R., et al. (2019). Cohesin-dependent regulation of gene expression during differentiation is lost in cohesin-mutated myeloid malignancies. Blood *134*, 2195-2208.

Sobhani, A., Khanlarkhani, N., Baazm, M., Mohammadzadeh, F., Najafi, A., Mehdinejadiani, S., and Sargolzaei Aval, F. (2017). Multipotent stem cell and current application. Acta Med. Iran. *55*, 6-23.

Sofueva, S., Yaffe, E., Chan, W.C., Georgopoulou, D., Vietri Rudan, M., Mira-Bontenbal, H., Pollard, S.M., Schroth, G.P., Tanay, A., and Hadjur, S. (2013). Cohesin-mediated interactions organize chromosomal domain architecture. EMBO J. *32*, 3119-3129.

Steinbeck, J.A. and Studer, L. (2015). Moving stem cells to the clinic: potential and limitations for brain repair. Neuron *86*, 187-206.

Subramanian, V., Klattenhoff, C.A., and Boyer, L.A. (2009). Screening for novel regulators of embryonic stem cell identity. Cell Stem Cell *4*, 377-378.

Suzuki, S., Namiki, J., Shibata, S., Mastuzaki, Y., and Okano, H. (2010). The neural stem/progenitor cell marker nestin is expressed in proliferative endothelial cells, but not in mature vasculature. J. Histochem. Cytochem. *58*, 721-730.

Takahashi, K. and Yamanaka, S. (2006). Induction of pluripotent stem cells from mouse embryonic and adult fibroblast cultures by defined factors. Cell *126*, 663-676.

Takigawa, M. (2013). CCN2: a master regulator of the genesis of bone and cartilage. J. Cell Commun. Signal. *7*, 191-201.

Vazin, T. and Freed, W.J. (2010). Human embryonic stem cells: derivation, culture, and differentiation: a review. Restor. Neurol. Neurosci. *28*, 589-603.

Viny, A.D., Bowman, R.L., Liu, Y., Lavallée, V.P., Eisman, S.E., Xiao, W., Durham, B.H., Navitski, A., Park, J., Braunstein, S., et al. (2019). Cohesin members Stag1 and Stag2 display distinct roles in chromatin accessibility and topological control of HSC self-renewal and differentiation. Cell Stem Cell *25*, 682-696.e8.

Walker, E., Ohishi, M., Davey, R.E., Zhang, W., Cassar, P.A., Tanaka, T.S., Der, S.D., Morris, Q., Hughes, T.R., Zandstra, P.W., et al. (2007). Prediction and testing of novel transcriptional networks regulating embryonic stem cell self-renewal and commitment. Cell Stem Cell *1*, 71-86.

Willerth, S.M., Arendas, K.J., Gottlieb, D.I., and Sakiyama-Elbert, S.E. (2006). Optimization of fibrin scaffolds for differentiation of murine embryonic stem cells into neural lineage cells. Biomaterials *27*, 5990-6003.

Xu, B., Bai, Z., Yin, J., and Zhang, Z. (2019). Global transcriptomic analysis identifies SERPINE1 as a prognostic biomarker associated with epithelial-to-mesenchymal transition in gastric cancer. PeerJ *7*, e7091.

Young, R.A. (2011). Control of the embryonic stem cell state. Cell *144*, 940-954.

Zakrzewski, W., Dobrzyński, M., Szymonowicz, M., and Rybak, Z. (2019). Stem cells: past, present, and future. Stem Cell Res. Ther. *10*, 68.

Zhang, H. and Wang, Z.Z. (2008). Mechanisms that mediate stem cell self-renewal and differentiation. J. Cell. Biochem. *103*, 709-718.